Beam-Beam Deflection and Beamstrahlung Monitor Response for Tilted Elliptic Beams*

V. Ziemann
Stanford Linear Accelerator Center, Stanford University, Stanford, CA 94309

ABSTRACT

At the interaction point of the SLC two oppositely running bunches with energies of 46 GeV and transverse extensions of a few microns are brought into collision. The strong electric and magnetic fields produced by one bunch lead to a deflection of the other bunch and to the emission of synchrotron radiation of critical energies of a few 10 MeV. This radiation, coined beamstrahlung, is detected in a Čerenkov monitor. In this paper a simulation code for the beam-beam interaction of two tilted elliptic beams is presented. A closed expression for the deflection angles is presented and the number of generated Čerenkov photons is calculated.

INTRODUCTION

At the interaction point of the SLC electron and positron bunches with a few times 10^{10} particles and bunch lengths of about 1 mm collide head on. This large number of particles in that small volume gives rise to large electromagnetic fields that the bunch carries along. Peak values of the magnetic fields in excess of 10 T occur which deflect the particles in the oppositely running bunch with deflection angles of up to 200 μrad. The effect of the fields can be characterized by a *local bending radius* ρ by which the oncoming particles are deflected. It is given by [1]

$$\frac{1}{\rho(x,y,t)} = |\Theta(x,y)|\frac{1}{\sqrt{2\pi}\sigma_z/2}\exp\left[-\frac{(ct)^2}{2(\sigma_z/2)^2}\right] , \quad (1)$$

where $\Theta(x,t)$ is the integrated deflection angle on the passage through the target bunch of length σ_z as is obvious from $|\Theta(x,y)| = \int_{-\infty}^{\infty} c\,dt/\rho(x,y,t)$. Thus the total deflection angle $\Theta(x,y)$ does not depend on the bunch length σ_z, but ρ does.

All transverse dependence of the deflection angle is buried in $\Theta(x,y)$, which for a general elliptic beam, characterized by its covariance matrix σ_{ij}, is given by [1]

$$\Theta(x,y) = \Delta y' + i\Delta x' = -\frac{2N_t r_e}{\gamma_r} F(x,y,\sigma_{ij}) , \quad (2)$$

$$F(x_1,x_2,\sigma_{ij}) = \frac{\sqrt{\pi}}{\sqrt{2(\sigma_{11}-\sigma_{22}+2i\sigma_{12})}}$$

$$\times\left\{w\left[\frac{x_1+ix_2}{\sqrt{2(\sigma_{11}-\sigma_{22}+2i\sigma_{12})}}\right] - e^{-\frac{1}{2}\sum_{i,j}^{2}(\sigma^{-1})_{ij}x_i x_j}\right.$$

$$\left.\times\, w\left[\frac{(\sigma_{22}-i\sigma_{12})x_1 + i(\sigma_{11}+i\sigma_{12})x_2}{\sqrt{\sigma_{11}\sigma_{22}-\sigma_{12}^2}\sqrt{2(\sigma_{11}-\sigma_{22}+2i\sigma_{12})}}\right]\right\} , \quad (3)$$

where N_t is the number of particles in the target beam and γ_r is the energy of the deflected particle in units of the electrons rest mass.

* Work supported in part by Department of Energy contract DE-AC03-76SF00515

U.S. Government work not protected by U.S. Copyright.

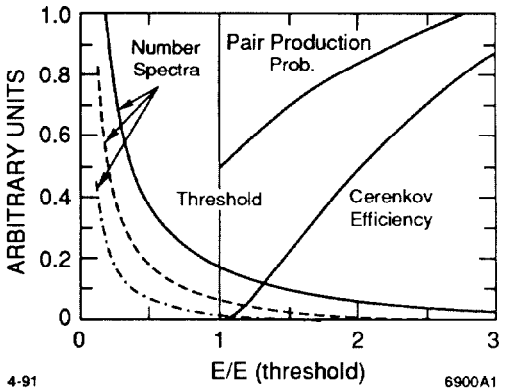

Figure 1. The pair production probability, Čerenkov photon generation efficiency and photon number spectra with critical energies of 1/2 (dotdashed), 1 (dashed) and 2 times (solid) the Čerenkov threshold. The vertical bar at 1 marks the Čerenkov threshold.

The bending radius $\rho(x,y,t)$ a particle experiences on its traversal of the oncoming bunch determines the spectrum of the emitted beamstrahlung, which is characterized by its critical energy $\varepsilon_c = 3\hbar c\gamma^3/(2\rho)$. Thus the number of beamstrahlung photons emitted per unit time and unit energy interval is given by [2]

$$\frac{dN}{d\varepsilon\,dt}\{\varepsilon,\varepsilon_c[\rho(t)]\} = \frac{1}{\sqrt{3}\pi}\frac{\alpha^2}{r_e mc}\frac{1}{\gamma^2}\int_{\varepsilon/\varepsilon_c}^{\infty} ds\, K_{5/3}(s) , \quad (4)$$

where $K_{5/3}$ is a Bessel function of fractional order [3]. Clearly, the emitted beamstrahlung spectrum depends on the local bending radius the radiating particle experiences through the critical energy ε_c. Of course the "hardest" spectrum is emitted when the bending radius is minimum at the core of the target bunch, whereas in the tails only a "soft" spectrum is emitted. Apparently, the spectrum varies as the radiating bunch traverses the target bunch. Photon number spectra for different critical energies are shown in Fig. 1.

THE BEAMSTRAHLUNG MONITOR

The beamstrahlung emanating from the interaction point is detected by a monitor about 40 m downstream. The monitor is also exposed to the radiation of a strong bending magnet and has to discriminate the photons generated in the bending magnet with critical energies of 2 MeV from the fewer photons generated in the beam-beam interaction with critical energies an order of magnitude larger.

The beamstrahlung monitor consists of a converter plate that converts the incident photons into e^+e^- pairs. This probability is given by the Heitler-Sauter cross section [4] for $\gamma \to e^+e^-$ processes which has a logarithmic dependence on the energy of the incident photon.

The generated e^+e^- pairs then travel through a gas volume made of ethylene at 1/3 atmosphere where they emit Čerenkov light. The Čerenkov photons are subsequently passed through a light channel by mirrors and are then detected by photo multiplier tubes. The threshold energy is determined by the gas and is about 25 MeV for the current monitor which leads to a $\gamma_0 \approx 50$. In Refs. [1, 5] it was shown that the number of Čerenkov photons depends on the energy of the incident photon γ_B simply according to $(1/\gamma_0 - 1/\gamma_B)^2$, as shown in Fig. 1 by the lower curve starting at the threshold. Here the energy of the photon γ_B is given in units of electron rest mass.

In order to determine how many Čerenkov photons are produced from the incident radiation characterized by its critical energy ε_c we have to integrate the number spectrum of incident photons weighted by the e^+e^- pair production probability and the probability of emitting a Čerenkov photon. This calculation has to be done for different critical energies in order to obtain a relation between the local bending radius and the number of generated Čerenkov photons per unit time [1]

$$\frac{dN_c}{dt}(x,y,t) = \Omega_0 I_0(\varepsilon_0, \varepsilon_c(x,y,t)) \ , \qquad (5)$$

where Ω_0 contains all the information about the hardware of the Čerenkov monitor. $I_0(\varepsilon_0, \varepsilon_c)$ is given by a complicated integral that is numerically evaluated in Ref. [1]. I_0 vanishes rapidly for small $\varepsilon_c/\varepsilon_0$ due to the decreasing tail of the "soft" spectrum emitted by the particles while they traverse the tails of the target beam.

From the dependence of I_0 on $\varepsilon_c/\varepsilon_0$ we can deduce scaling relations for the beamstrahlung flux. It turns out [1] that $I_0 \propto (\varepsilon_c/\varepsilon_0)^4$ for $\varepsilon_c/\varepsilon_0 \lesssim 0.7$. Since $\varepsilon_c \propto 1/\rho$ we can use Eqs. (1)-(2) and obtain the following scaling relation for the number of Čerenkov photons

$$\int \frac{dN_c}{dt} dt \propto \frac{N_{target}^4 N_{source}}{\sigma_z^3 \gamma_{source}^4} |F(x,y,\sigma_{ij})|^4 \ , \qquad (6)$$

where all transverse dependence is buried in the function F, defined in Eq. (3).

The Simulation Algorithm

Using Eq. (5), it is easy to calculate the total number of Čerenkov photons generated during a collision by integrating dN_c/dt over t, and averaging over the transverse dimensions x and y

$$N_c = \int_{-\infty}^{\infty} dx \int_{-\infty}^{\infty} dy \, \psi_r(x,y) \int_{-\infty}^{\infty} dt \, \frac{dN_c}{dt}(x,y,t) \ , \qquad (7)$$

where $\psi_r(x,y)$ is the transverse particle distribution of the radiating beam, assumed to be Gaussian with centroid position X_i and covariance matrix $\tilde{\sigma}_{ij}$. dN_c/dt depends on the target beam distribution through the dependence of the critical energy ε_c on the local bending radius $\rho(x,y,t)$, as given by Eq. (1).

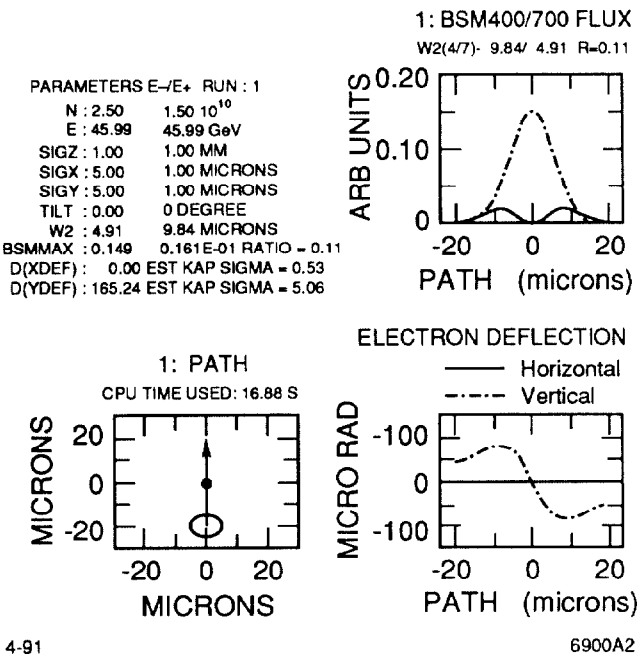

Figure 2. A typical output from the simulation code. In the upper left the input data are echoed. In the upper right the beamstrahlung fluxes are shown in arbitrary units. The solid curve is the flux from the radiating positrons on the north monitor. In the lower left depicts the path on which the scan was taken and the lower right shows the electron deflection. Here the solid curve shows the horizontal deflection and the dashed curve the vertical.

The seemingly necessary three integrations can be reduced to two by expanding I_0 into a power series in ρ_0/ρ. Using this expansion, the integral over t can be done analytically, and only two spatial integrations remain which then have to be evaluated numerically.

The beam-beam deflection angle for the centroid kick is given by the average of the deflection angle over the distribution of the kicked particles. It was evaluated in Ref. [1] in closed form, and can be written as

$$\langle \Theta \rangle = -\frac{2N_t r_e}{\gamma_r} F(X_1, X_2, \Sigma_{ij}) \ , \qquad (8)$$

where N_t is the number of particles in the target beam, and γ_r the energy of the radiating beam in units of the electron rest mass. X_1 and X_2 are the relative offsets in x and y, and Σ_{ij} is the sum of the covariance matrices of the target and the deflected beam. Since only the sum of the beam sizes appears in Eq. (8), it is not possible to determine individual beam sizes from beam-beam deflections independently.

The simulation code calculates both the deflection angles and the beamstrahlung fluxes for points along a straight path that has to be specified by the user. Fig. 2 shows typical output of the code. The simulation of a typical beam-beam scan with 40 data points in which both beamstrahlung scans and the deflection curves are calculated takes about 60 s.

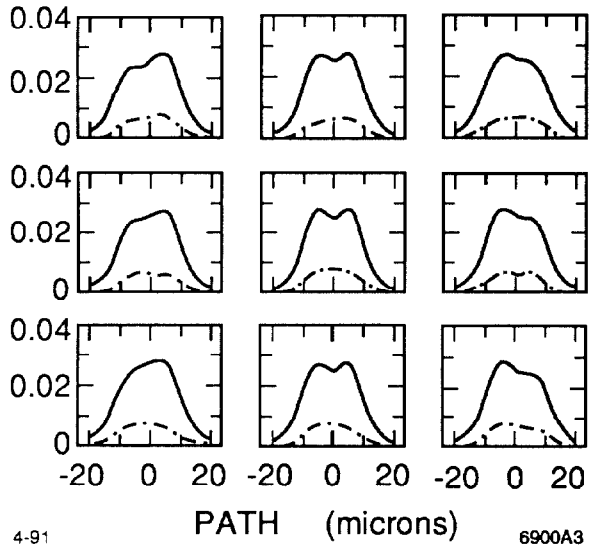

Figure 3. Vertical beamstrahlung scans for tilted beams offset with respect to each other. The beam sizes for both beams are 5×3 μm. The tilt angle is -45, 0 and $+45$ degree with respect to the horizontal axis from left to right for the positrons and top to bottom for electrons.

Round Beams

Fig. 2 shows the result where a large electron beam with $\sigma_r = 5$ μm is passed over a small positron beam with $\sigma_r = 1$ μm. The extrema of the beamstrahlung flux from the small e^+ beam (solid) coincide with the extrema of the deflection curve, because there the local bending radius the e^+ experience is largest. The deflection near the center of the target e^- beam is weaker and causes the dip. For an ideal point like e^+ source beam the dip should decrease to zero.

The radiation from the electrons (dotdashed) reflects mainly the transverse distribution of the electron beam, because only those e^- radiate that are intercepted by the fields of the positron beam, which serves as a window to view the radiating electrons.

Simulations with varying bunch sizes of 3, 4, and 5 μm for electrons and positrons confirmed the above observation [1] that the dip is always associated with the larger target beam size. This fact can be exploited as a diagnostic tool.

Tilted Elliptic Beams

At first sight it appears obvious to associate asymmetric beamstrahlung scans with tilted beams. However, if the scan is centered, the beamstrahlung scans are still symmetric, because the configuration shortly before the source beam enters the target beam is (point-) symmetric to that shortly after it exits. Therefore the fluxes are the same.

In order to break this symmetry and examine the $x-y$ coupling we have to offset the beams with respect to each other. Fig. 3 shows the results where tilted beams are scanned with 3 μm offset. Clearly now asymmetric scans are produced.

These observations can prove to be useful to diagnose tilted beams, however, only if the beams are known to be of equal size is it possible to determine the tilt direction of the individual beams [1].

Conclusions

A simulation code for the experimentally observable effects of beam-beam deflection and beamstrahlung at SLC final focus is described. In the code the interaction of general Gaussian particle distributions in the non-disruptive regime is simulated.

The simulations show that the dip in beamstrahlung scans is associated with a larger target beam size compared to the beam size of the radiating beam. Asymmetric scans turn out to be related to tilted beams that are scanned across each other with an offset.

The simulations show that it is possible to assess individual beam sizes with beamstrahlung scans whereas this is in principle not possible with deflection scans. Work based on Ref. [6] is in progress to utilize the simulation code and determine individual beam sizes quantitatively.

In the near future we hope to use these results as tools to diagnose the beams at the SLC final focus.

Acknowledgements

Discussions with C. Field and N. Toge are gratefully acknowledged. In particular discussions with E. Gero, who wrote his thesis on this subject were very helpful.

References

[1] V. Ziemann, SLAC Collider Note CN-384, 1990.

[2] A. Sokolov, I. Ternov, *Synchrotron Radiation,* Pergamon Press, New York, 1968.

[3] M. Abramowitz, I. Stegun, *Handbook of Mathematical Functions,* Dover, New York, 1972.

[4] J. Motz, H. Olsen, H. Koch, Rev. Mod. Phys. **41**, 581, 1969.

[5] P. Chen, SLAC AAS-Note 40, 1988.

[6] E. Gero, Ph.D. Thesis, Univ. of Michigan, 1991.